Supplementary Information

Mesoporous Silica Nanoparticles-Embedded Lanthanide Organic Polyhedra for Enhanced Stability, Luminescence and Cell Imaging†

Xiao-Shan Lin, [a, b] Yanzi Yu,[c] Li-Peng Zhou,*[a,b], Lizhen He,*[c] Tianfeng Chen,[c] and Qing-Fu Sun*[a, b]

[a]*College of Chemistry and Materials Science, Fujian Normal University, Fuzhou 350007, P. R. China. E-mail: qfsun@fjirsm.ac.cn; zhoulp@fjirsm.ac.cn*

[b]*State Key Laboratory of Structural Chemistry, Fujian Institute of Research on the Structure of Matter, Chinese Academy of Sciences, Fuzhou 350002, P. R. China*

[c]*Department of Neurology and Stroke Center, The First Affiliated Hospital and Department of Chemistry, Jinan University, Guangzhou 510632, P. R. China. E-mail: hlz6371@jnu.edu.cn.*

Contents

1. General

Unless otherwise stated, all chemicals and solvents were purchased from commercial companies and used without further purification. Triethanolamine (TEA), Cetyltrimethylammonium bromide (CTAB), tetraethoxysilane (TEOS), 3-aminopropyltriethoxysilane (APS), triethanolamine (TEOA), $Eu(OTf)_3$, D-biotin, 1-(3-dimethylaminopropyl)-3-ethylcarbodiimide (EDC), N-hydroxysuccinimide (NHS) were purchased from Adamas (Shanghai).

Thermogravimetric analysis (TGA) was investigated on a NETZSCH STA449F3 unit under N_2 atmosphere at a heating rate of 10 K min^{-1}. Nitrogen adsorption/ desorption isotherms were measured with an ASAP 2020 based on the Brunauer-Emmett-Teller (BET) method. Fourier transform infrared (FT-IR) spectra were recorded on the Bruker VERTEX70 system by mixing samples into KBr to prepare a compressed tablet sample. Inductively coupled plasma (ICP) analyses were performed on a Jobin Yvon Ultima2 spectrometer. The Zeta potentials of the hybrid nanoparticles were analyzed on a Malvern Nanosizer S instrument at room temperature. X-ray photoelectron spectroscopy (XPS) was conducted on a Thermo Fisher ESCALAB 250Xi by using an Al Kα (λ = 8Å, $h\nu$ =1486.6 eV) X-ray source without any etching. The morphology of the hybrid materials was characterized by Field emission scanning electron microscope (FESEM) on a SU-8010 operating and high resolution transmission electron microscope (HRTEM) on a FEI Tecnai F20 operating, respectively. UV-vis spectra are recorded on UV-2700 spectrophotometer from SHIMADZU. The excitation and emission spectra were collected by FS5 spectrofluorometer from Edinburg Photonics. The emission quantum yields in nanoparticles were measured on FS5 with a SC-30 Integrating Sphere.

2. Synthesis and Characterization

2.1 Synthetic procedures

The ligand (H_4L) and $(Et_4N)_{24}Eu_8L_{12}$ complex were synthesized according to the

reported method from our previous literature.[S1]

Synthesis of MSNs MSNs nanoparticles were synthesized by a modified method according to previous reports. Spherical MSNs with uniform diameter were prepared by base catalytic condensation. Briefly, CTAB (1.2 g, 3.3 mmol) and TEOA (3.3 mL, 0.27 mmol) were firstly added into 100 mL of deionized water and heated at 60℃ for 1 hour at a magnetic stirring rate of about 900 rpm. Then TEOS (8.4 mL) was added to the above reaction system drop by drop. Subsequently, the temperature was increased from 60 to 80 °C and stirring continued at 80 °C for 4 h. After centrifugation at 11000 rpm for 10 min, the crude products were further refluxed in the ethanol solution of sodium chloride (5 M) at 80 °C overnight to remove the template of CTAB. Repeat this procedure for three times. After centrifuging and washing with deionized water for three times, white powdery MSNs nanoparticles were obtained by freeze-drying.

Synthesis of Eu_8L_{12}@MSNs Mesoporous silica nanoparticles (100 mg) were suspended in cyclohexane (100 mL) and deionized water (20 mL), to which the DMSO solution of $Eu(OTf)_3$ (60 mg·mL^{-1}, 1 mL, 0.10 mmol) was added and vigorously stirred for 24 h at room temperature. Then, the fresh DMSO solution of $(Et_4N)_4L$ (mixing H_4L (20 mg, 0.03 mmol) with $(Et_4N)_4$·OH (25 wt.% in H_2O, 70 μL, 0.12 mmol) was added and further stirred at 50 °C for 24 h. Afterwards, the suspension was centrifuged and washed with deionized water for three times. After freeze-drying, the hybrid product Eu_8L_{12}@MSNs was obtained as a white powder.

Synthesis of Eu_8L_{12}@MSNs-NH_2 TEOS (100 μL) and APS (100 μL) were added into the solution of Eu_8L_{12}@MSNs (50 mg) in ethanol (100 mL) with vigorous stirring at room temperature for 24 hours. Then, the mixture was washed for three times with deionized water and collected by centrifugation. Finally, the white powder of amino-functional hybrid material Eu_8L_{12}@MSNs-NH_2 was obtained by freeze drying.

Synthesis of Eu_8L_{12}@MSNs-biotin EDC·HCl (40 mg, 0.21 mmol) and NHS (40 mg, 0.35 mmol) were added into a solution of biotin (20 mg, 0.09 mmol) in

DMSO (4 mL) and the mixture was stirred at room temperature for 2 hours. Then the activated biotin N-hydroxysuccinimide ester was directly added into a dispersion solution of Eu_8L_{12}@MSNs-NH_2 nanoparticles (50 mg) in deionized water (100 mL) and the mixture was vigorously stirred at room temperature for 24 hours. The resulting biotin-labeled nanoparticles of Eu_8L_{12}@MSNs-biotin were collected by centrifugating and following washing with deionized water for three times. A white powder was obtained after freeze-drying.

2.2 Characterization

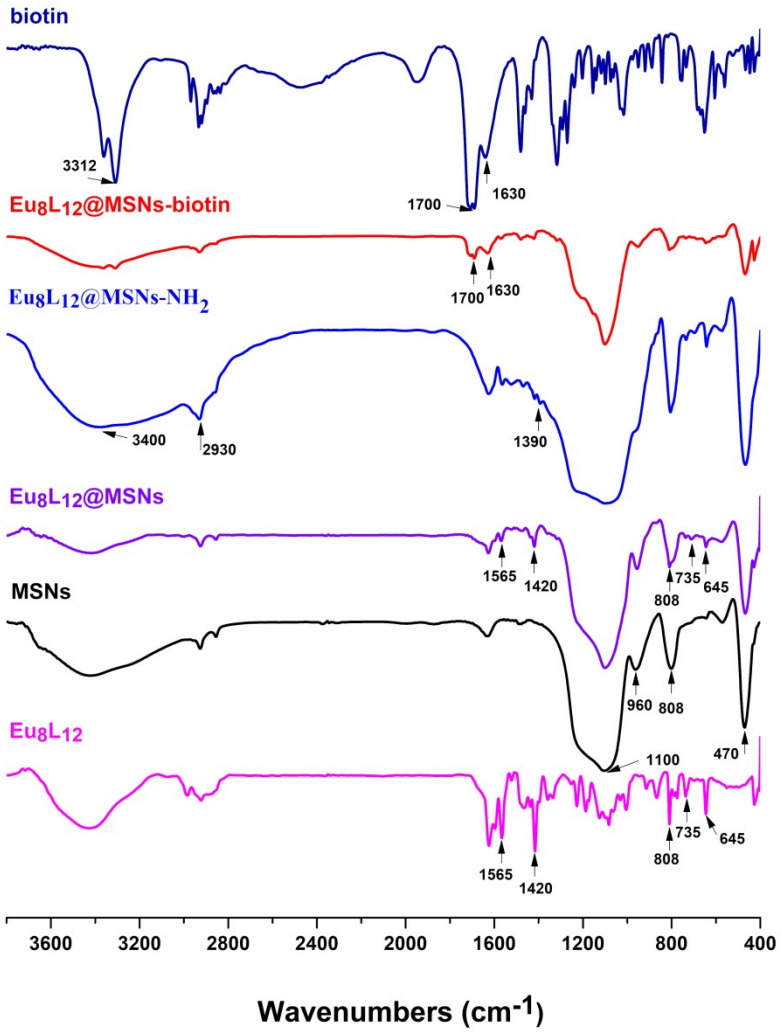

Figure S1. FT-IR spectra of Eu_8L_{12}, MSNs, Eu_8L_{12}@MSNs, Eu_8L_{12}@MSNs-NH_2, Eu_8L_{12}@MSNs-biotin, and biotin.

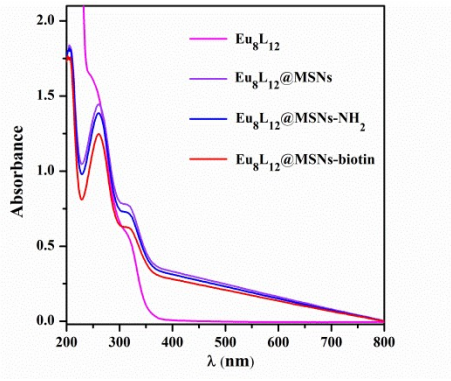

Figure S2. UV-vis absorption spectra of Eu_8L_{12} (1.667×10^{-6} M), Eu_8L_{12}@MSNs, Eu_8L_{12}@MSNs-NH_2 and Eu_8L_{12}@MSNs-biotin (0.125 mg/mL) in water.

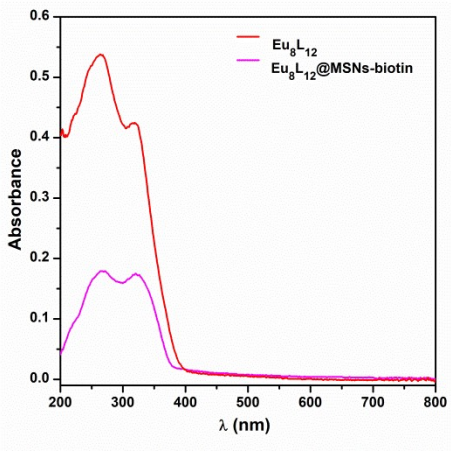

Figure S3. Solid state UV−vis spectra of Eu_8L_{12} and Eu_8L_{12}@MSNs-biotin.

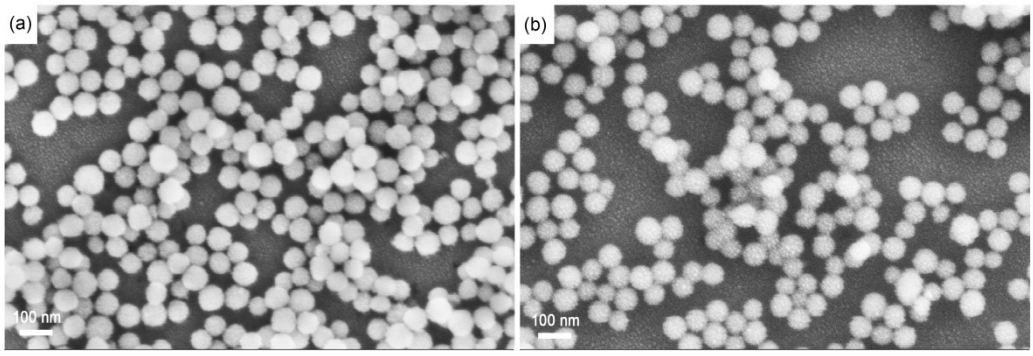

Figure S4. SEM of (a) Eu_8L_{12}@MSNs and (b) Eu_8L_{12}@MSNs-NH_2.

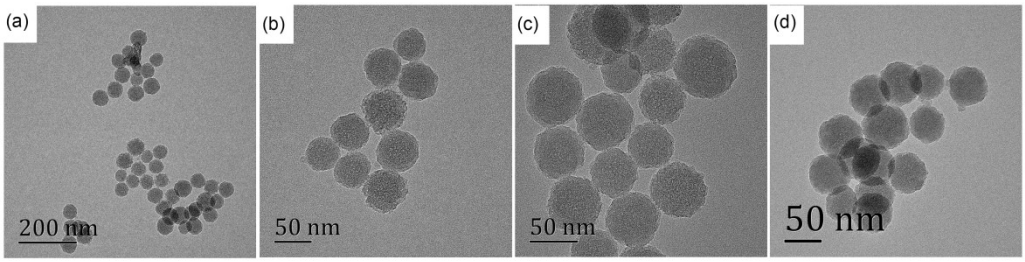

Figure S5. TEM of (a) MSNs, (b) Eu_8L_{12}@MSNs, (c) Eu_8L_{12}@MSNs-NH_2 and (d)

Eu_8L_{12}@MSNs-biotin.

2.3 Determination of the loading amount

The exact loading amounts of Eu_8L_{12} in hybrid materials were determined by an method of degradation.

To a fresh DMSO solution of $(Et_4N)_{24}Eu_8L_{12}$ (2 mg/mL referred to H_4L, 1 mL) was added KOH aqueous solution (1 M, 1 mL) and stirred at 50 ℃ for 24 h. This solution was diluted into different concentrations for UV-vis absorption testing. A standard calibration curve was plotted based on the UV-vis absorbance at 310 nm.

Similarly, 10 mg Eu_8L_{12}@MSNs was incubated in the mixture solution of DMSO (1 mL) and 1 M KOH aqueous solution (1 M, 1 mL) at 50℃ with stirring for 24 h and then diluted to 0.125 mg·mL^{-1} for UV-vis testing.

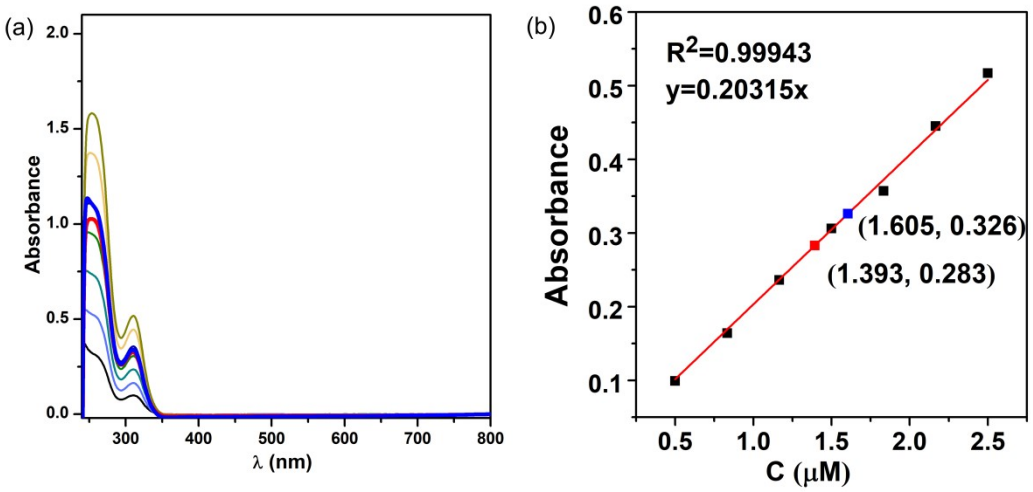

Figure S6. (a) UV-vis absorption spectra and of $(Et_4N)_{24}Eu_8L_{12}$ after degradation at different concentrations; (b) the standard curve based on the absorption at 310 nm (DMSO/KOH aq. (1 M), v/v =1:1, 298 K). The UV-vis absorption spectra of Eu_8L_{12}@MSNs-NH_2 and Eu_8L_{12}@MSNs-biotin after degradation were highlighted as blue curve (square) and red curve (square), respectively.

Table S1. The loading amount of Eu_8L_{12} in different hybrid materials.

	A_{310}[a]	C [b] (uM)	Loading (umol·g^{-1})
Eu_8L_{12}@MSNs	0.339	1.669	13.350
Eu_8L_{12}@MSNs-NH_2	0.326	1.605	12.838
Eu_8L_{12}@MSNs-biotin	0.283	1.393	11.145

[a] The concentrations of the hybrid materials for UV-vis testing were 0.125 mg·mL^{-1}.

[b] The concentrations of Eu_8L_{12} in UV-vis testing solution of different hybrid materials.

3. Photophysical property

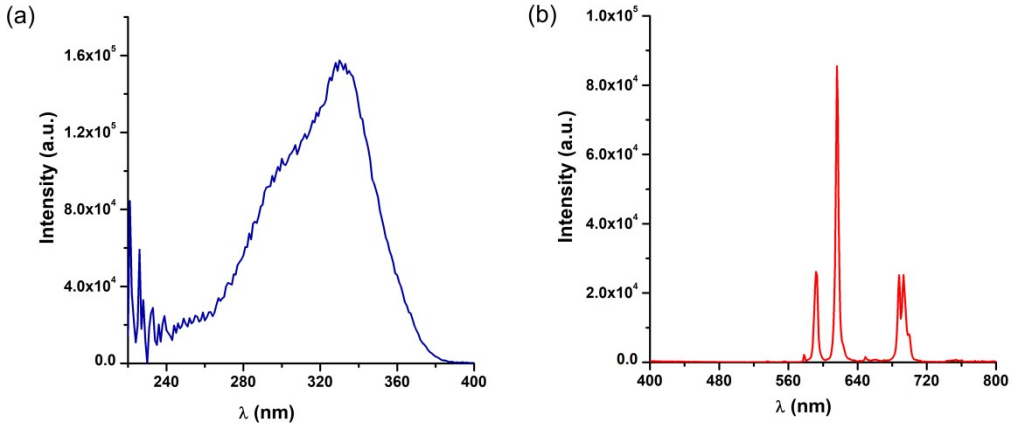

Figure S7. (a) Excitation (λ_{em} = 616 nm, slits = 0.5 - 0.5) and (b) emission (λ_{ex} =330 nm, slits = 1.0 – 1.0) spectra of Eu_8L_{12} (c = 1.667×10^{-6} M) in H_2O at 298 K.

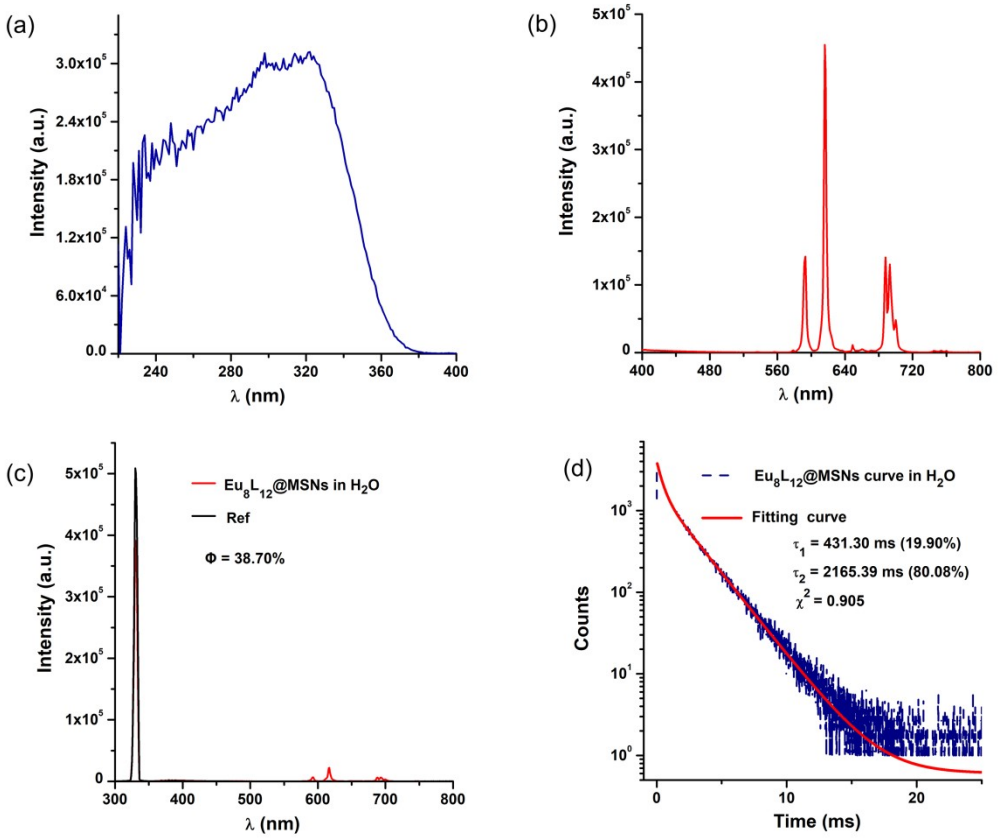

Figure S8. (a) Excitation spectrum (λ_{em} = 616 nm, slits = 0.5 - 0.5), (b) emission spectrum (λ_{ex} = 330 nm, slits=1.0 - 1.0), (c) quantum yield ($\Phi_{overall}$ = 38.70 %, λ_{ex} = 330 nm, slits = 6.0 - 0.6), and (d) excited state decay curve (λ_{ex} = 330 nm, slits = 2 - 0.5) of Eu_8L_{12}@MSNs (c = 0.125 mg·mL^{-1}) in H_2O at 298 K.

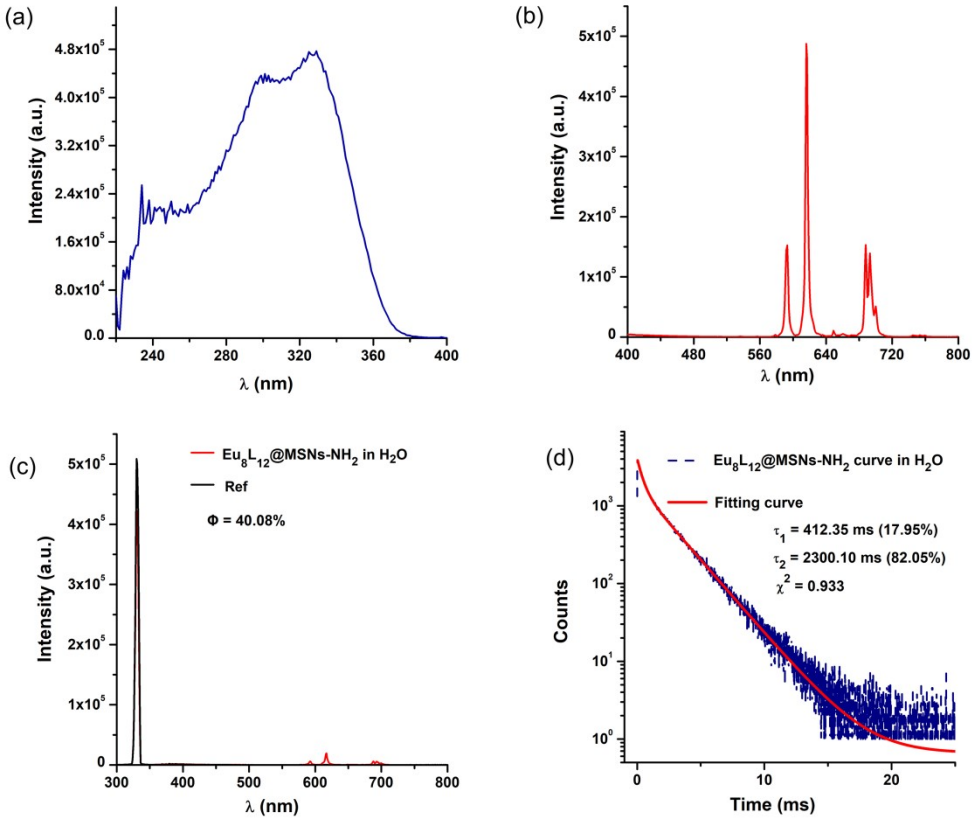

Figure S9. (a) Excitation spectrum (λ_{em} = 616 nm, slits = 0.5 - 0.5), (b) emission spectrum (λ_{ex} = 330 nm, slits=1.0 - 1.0), (c) quantum yield ($\Phi_{overall}$ = 40.08 %, λ_{ex} = 330 nm, slits = 6.0 - 0.6), and (d) excited state decay curve (λ_{ex} = 330 nm, slits = 2 - 0.5) of Eu_8L_{12}@MSNs-NH_2 (c = 0.130 mg·mL^{-1}) in H_2O at 298 K.

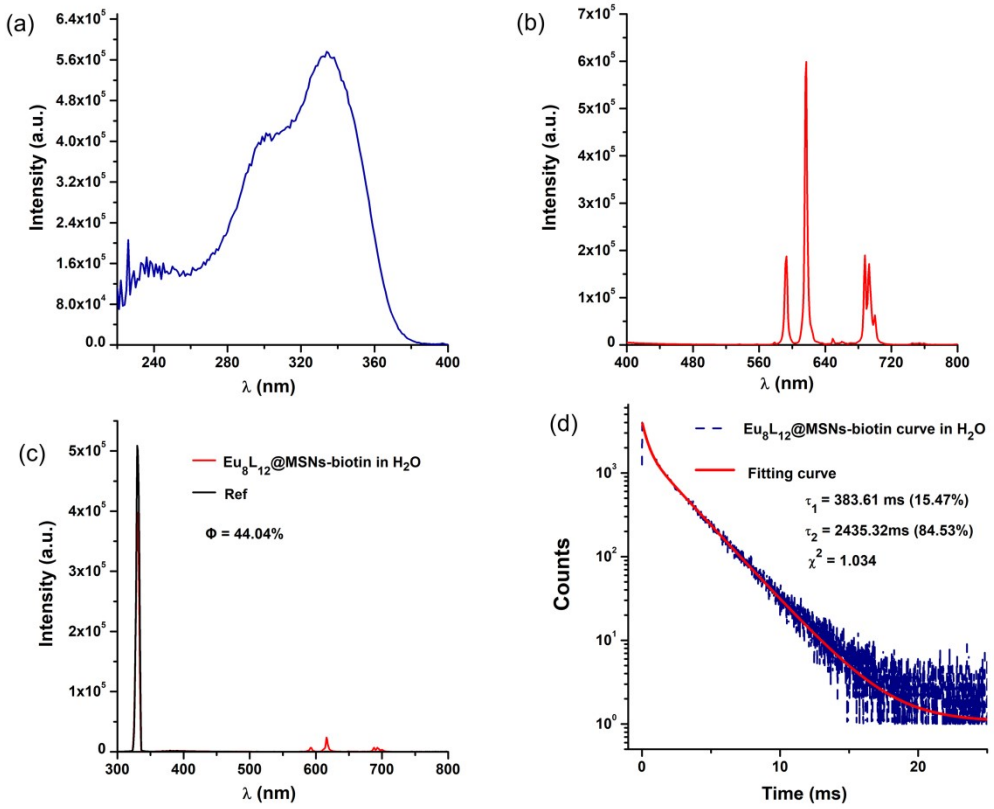

Figure S10. (a) Excitation spectrum (λ_{em} = 616 nm, slits = 0.5 - 0.5), (b) emission spectrum (λ_{ex} = 330 nm, slits=1.0 - 1.0), (c) quantum yield ($\Phi_{overall}$ = 44.04 %, λ_{ex} = 330 nm, slits = 6.0 - 0.6), and (d) excited state decay curve (λ_{ex} = 330 nm, slits = 2 - 0.5) of Eu_8L_{12}@MSNs-biotin (c = 0.150 mg·mL^{-1}) in H_2O at 298 K.

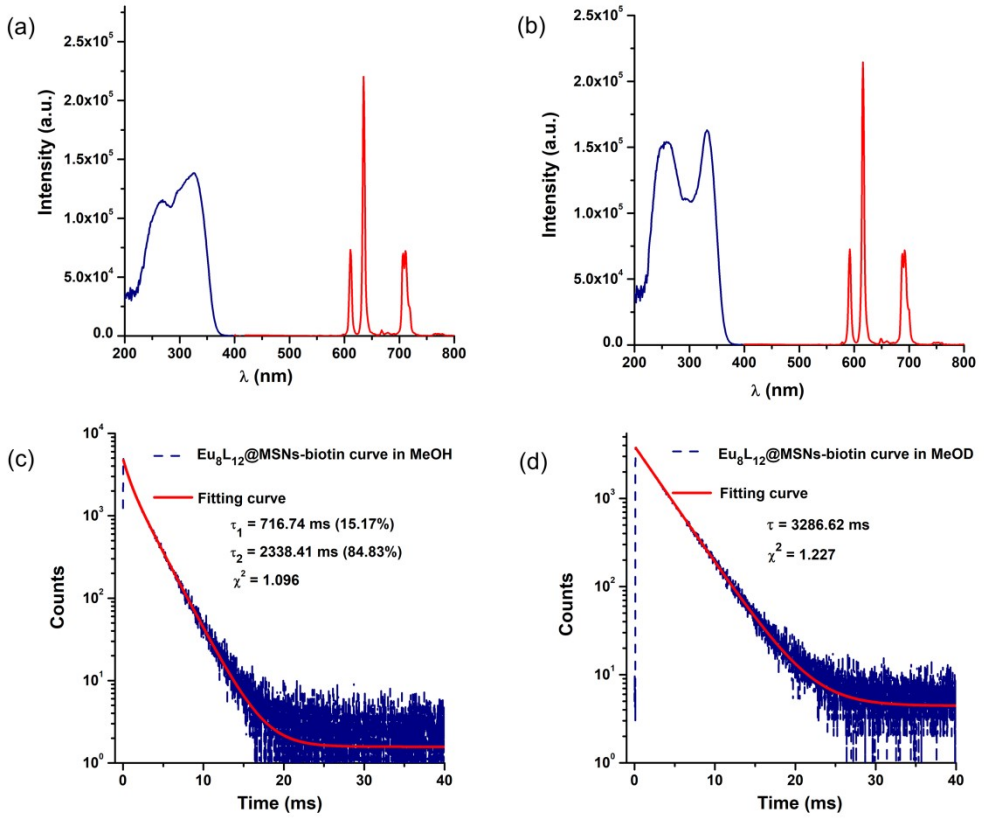

Figure S11. Excitation (blue lines, λ_{em} = 616 nm, slits = 2.5 - 3) and emission (red lines, λ_{ex} =330 nm, slits = 3.5 - 4) spectra of Eu_8L_{12}@MSNs-biotin (c = 0.3 mg·mL^{-1}) in MeOH (a) and in MeOD (b); excited state decay curve for Eu_8L_{12}@MSNs-biotin in MeOH (c) and MeOD (d) (λ_{ex} =330 nm, slits = 3 - 3) at 298 K.

4. The stability of hybrid materials

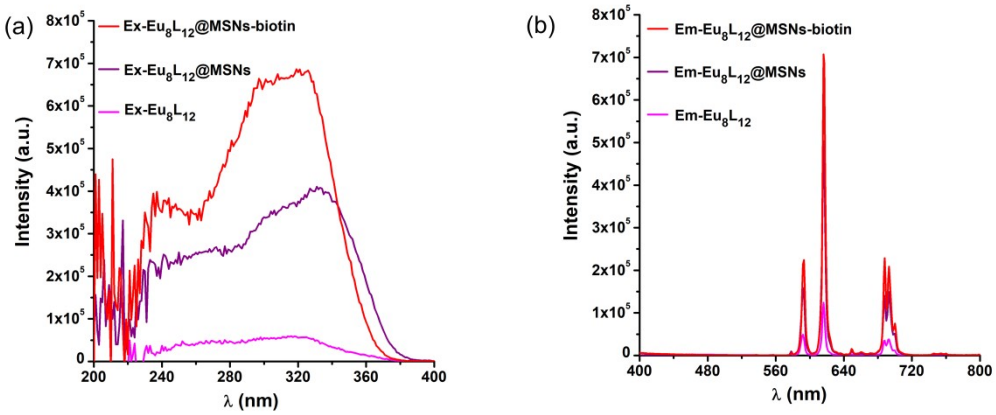

Figure S12. (a) Excitation (λ_{em} = 616 nm, slits = 0.5 - 0.8) and (b) emission (λ_{ex} = 330 nm, slits=1.0 - 1.5) spectra of Eu_8L_{12} (c = 4.167 μM), Eu_8L_{12}@MSNs (c = 0.3 mg·mL^{-1}) and Eu_8L_{12}@MSNs-biotin (c = 0.3 mg·mL^{-1}) in HCl (pH = 4) at 298 K.

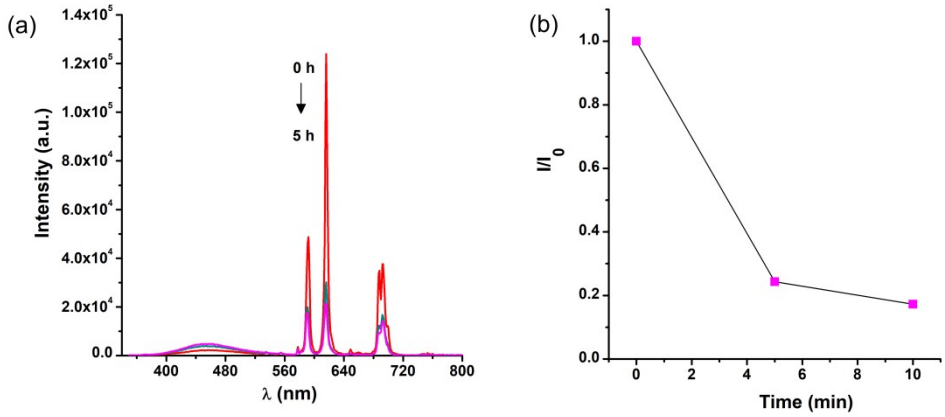

Figure S13. (a) Emission (λ_{ex}=330 nm, slits = 1.0 – 1.5) spectra and (b) emission attenuation of Eu_8L_{12} at 616 nm (c = 0.3 mg·mL^{-1}) in HCl (pH = 4) at 298 K.

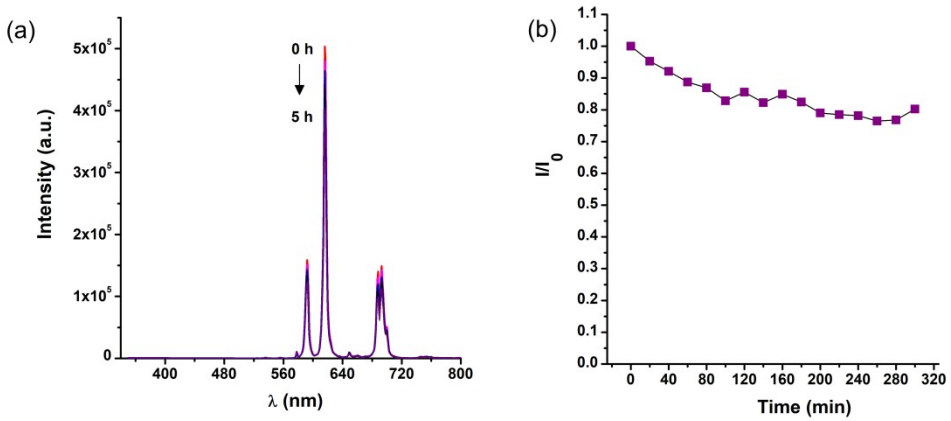

Figure S14. (a) Emission (λ_{ex}=330 nm, slits = 1.0 – 1.5) spectra and (b) emission attenuation of Eu_8L_{12}@MSNs at 616 nm (c = 0.3 mg·mL^{-1}) in HCl (pH = 4) at 298 K.

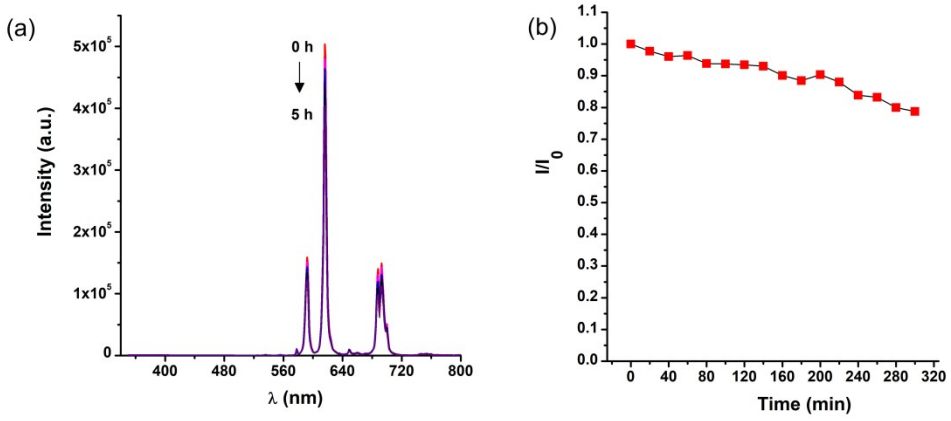

Figure S15. (a) Emission (λ_{ex}=330 nm, slits = 1.0 – 1.5) spectra and (b) emission attenuation of Eu_8L_{12}@MSNs-biotin at 616 nm (c =0.3 mg·mL^{-1}) in HCl (pH = 4) at 298 K.

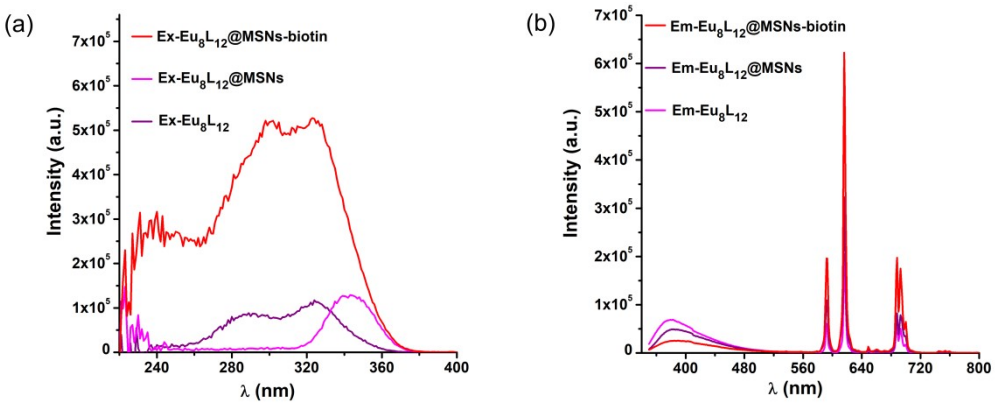

Figure S16. (a) Excitation (λ_{em} = 616 nm, slits = 0.5 - 0.8) and (b) emission (λ_{ex} = 330 nm, slits=1.0 - 1.5) spectra of Eu_8L_{12} (c = 4.167 μM), Eu_8L_{12}@MSNs (c = 0.3 mg·mL^{-1}) and Eu_8L_{12}@MSNs-biotin (c = 0.3 mg·mL^{-1}) in PBS (pH = 7.4, 10 mM Na_2HPO_4, 2 mM KH_2PO_4) at 298 K.

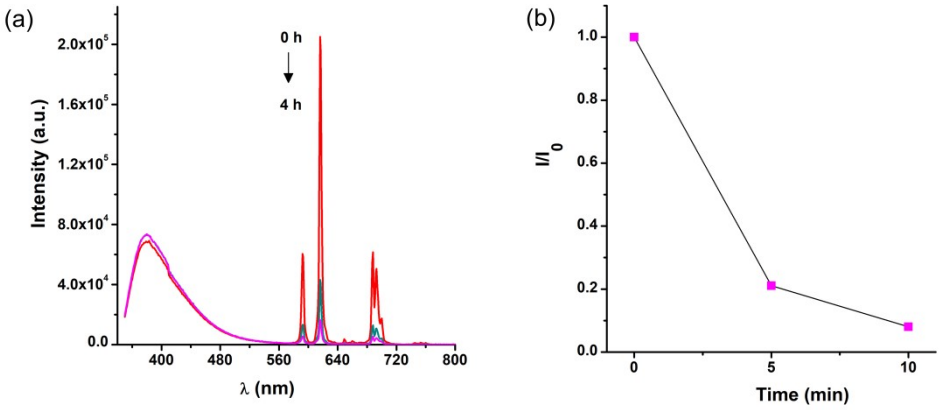

Figure S17. (a) Emission (λ_{ex}=330 nm, slits = 1.0 – 1.5) spectra and (b) emission attenuation of Eu_8L_{12} at 616 nm (c = 0.3 mg·mL^{-1}) in PBS (pH = 7.4, 10 mM Na_2HPO_4, 2mM KH_2PO_4) at 298 K.

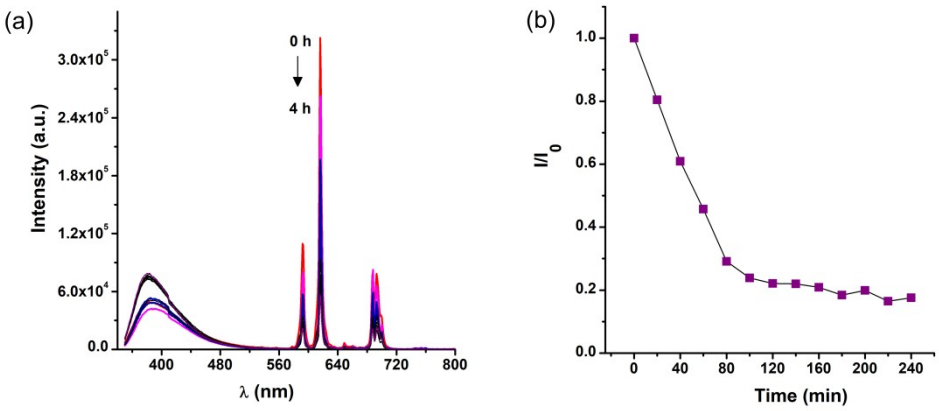

Figure S18. (a) Emission (λ_{ex}=330 nm, slits = 1.0 – 1.5) spectra and (b) emission attenuation of Eu_8L_{12}@MSNs at 616 nm (c = 0.3 mg·mL^{-1}) in PBS (pH = 7.4, 10 mM Na_2HPO_4, 2mM KH_2PO_4) at 298 K.

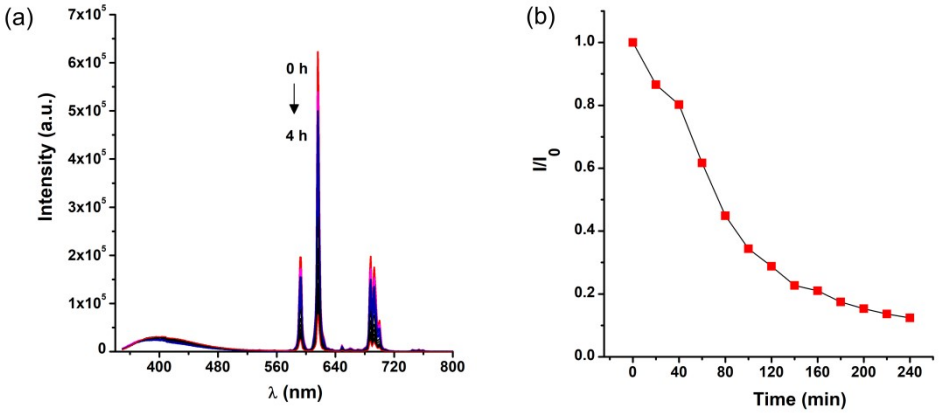

Figure S19. (a) Emission (λ_{ex}=330 nm, slits = 1.0 – 1.5) spectra and (b) emission attenuation of Eu_8L_{12}@MSNs-biotin at 616 nm (c = 0.3 mg·mL^{-1}) in PBS (pH = 7.4, 10 mM Na_2HPO_4, 2mM KH_2PO_4) at 298 K.

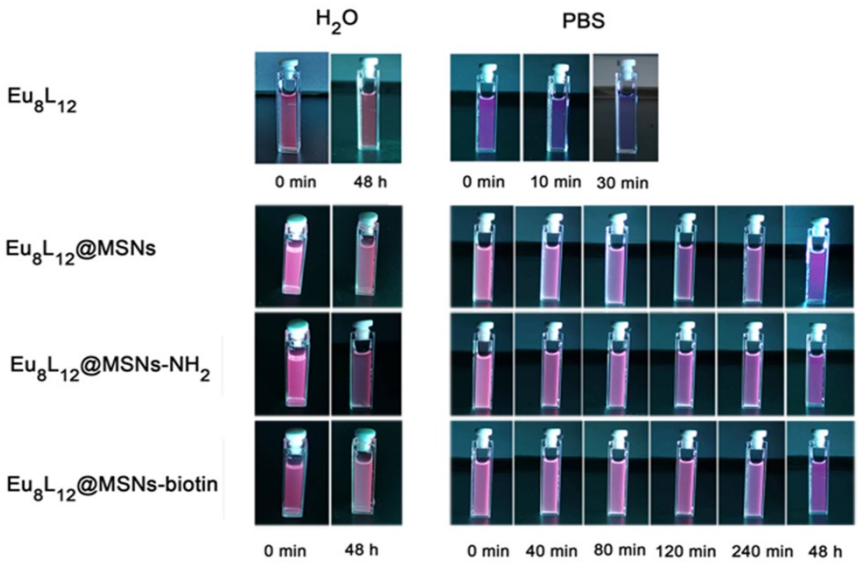

Figure S20. Digital photographs of (1.667 μM), Eu_8L_{12}@MSNs (0.125 mg·mL^{-1}), Eu_8L_{12}@MSNs-NH_2 (0.130 mg·mL^{-1}) and Eu_8L_{12}@MSNs-biotin (0.150 mg·mL^{-1}) dispersed in water and PBS (pH = 7.4, 10 mM Na_2HPO_4, 2 mM KH_2PO_4) for varied duration time under the irradiation of ultraviolet lamp at 365 nm.

5. Tumor-Targeted Imaging

The cell viabilities of MDA-MB-231 human breast cancer cells treated with different concentrations of Eu_8L_{12}, MSNs, Eu_8L_{12}@MSNs, Eu_8L_{12}@MSNs-NH_2, and Eu_8L_{12}@MSNs-biotin for 72 h have been evaluated by MTT assay.

Table S2. IC_{50} value of the hybrid materials towards MDA-MB-231 cancer cells.

	cisplatin	**Eu_8L_{12}**	**Eu_8L_{12}@SiO$_2$**	**Eu_8L_{12}@SiO$_2$-APS**	**Eu_8L_{12}@SiO$_2$-Biotin**
IC_{50}(μg·mL^{-1})	1.4	>80	21.7	45.1	24.9

MDA-MB-231 human breast cancer cells were used to evaluate the living cell imaging of the hybrid materials. Briefly, MDA-MB-231 human breast cancer cells were seeded in 2 cm petri dish and attached for 24 h. Then the cells were incubated with different concentration of hybrid materials for 24 h, and captured with fluorescence microscope (Cytation 5, BioTek Instruments, Inc.).

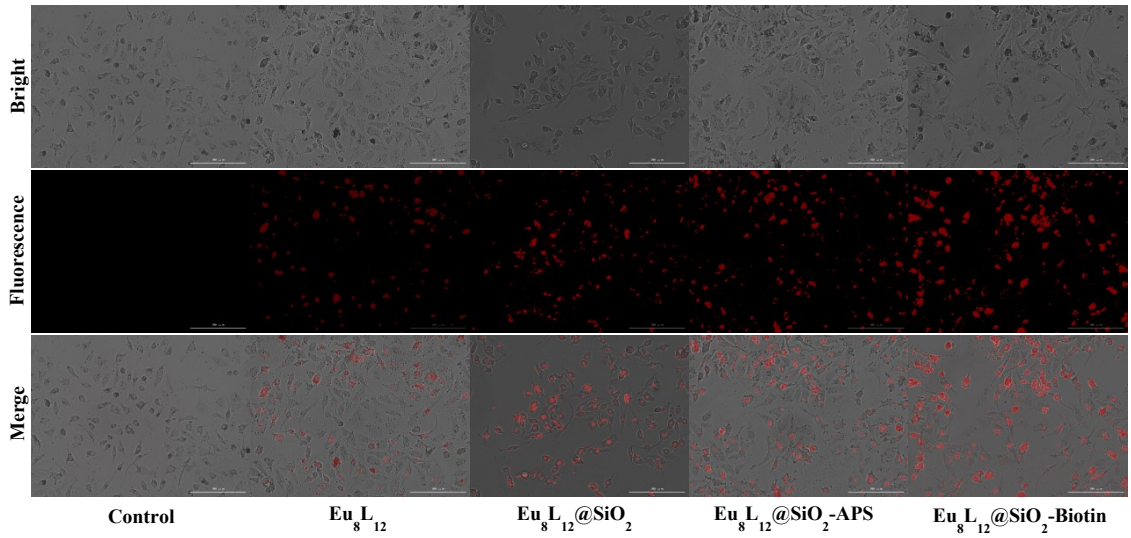

Figure S21. Confocal microscope images of MDA-MB-231 human breast cancer cells co-incubated with Eu_8L_{12}, Eu_8L_{12}@MSNs, Eu_8L_{12}@MSNs-NH_2 and Eu_8L_{12}@MSNs-biotin (5 μM referred to the complex), respectively.

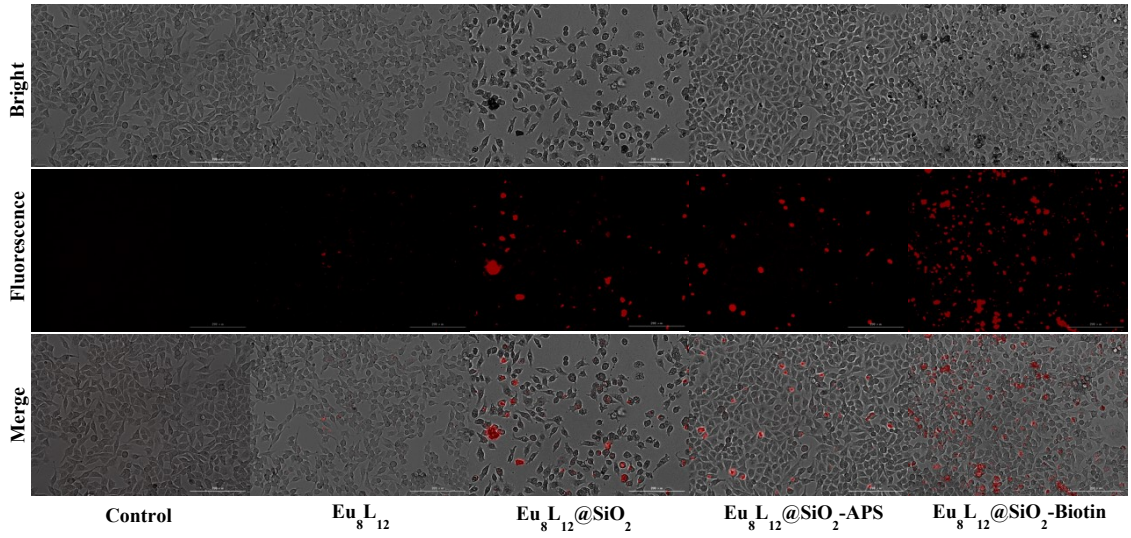

Figure S22. Confocal microscope images of MDA-MB-231 human breast cancer cells co-incubated with Eu_8L_{12}, Eu_8L_{12}@MSNs, Eu_8L_{12}@MSNs-NH_2 and Eu_8L_{12}@MSNs-biotin (0.4 μM referred to the complex), respectively.

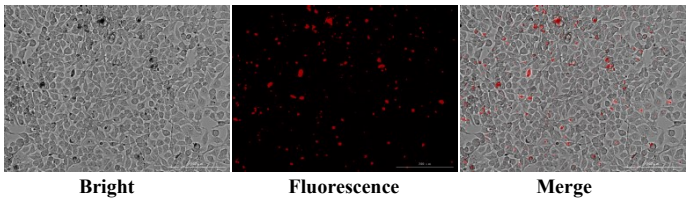

Figure S23. Confocal microscope images of MDA-MB-231 human breast cancer cells co-incubated with Eu_8L_{12}@MSNs-biotin (0.2 μM referred to the complex).

Table S3. Intracellular uptake percentages of Eu_8L_{12}@MSNs-biotin in MDA-MB-231 cancer cells and NIH 3T3 mouse fibroblasts cell.[a]

	MDA-MB-231	NIH 3T3
Intracellular uptake (%)	41	32

[a] MDA-MB-231 human breast cancer cells and NIH 3T3 mouse fibroblasts cells were incubated for 4 h in the presence of Eu_8L_{12}@MSNs-biotin (2.0 μM), respectively.

6. References

[S1] Z. Wang, L. Z. He, B. Q. Liu, L.-P. Zhou, L.-X. Cai, S.-J. Hu, X.-Z. Li, Z. Li, T. F. Chen, X. P. Li, and Q.-F. Sun, *J. Am. Chem. Soc.* **2020**, *142*, 16409.